ELSEVIER

Journal of Power Sources 104 (2002) 181–189

JOURNAL OF POWER SOURCES

www.elsevier.com/locate/jpowsour

Preparation of creep-resistant Ni–5 wt.% Al anodes for molten carbonate fuel cells

Gyubeom Kim*, Youngjoon Moon, Dokyol Lee

Division of Materials Science and Engineering, Korea University, 5-1 Anam-Dong, Sungbuk-Ku, Seoul 136-701, South Korea

Received 5 June 2001; accepted 21 August 2001

Abstract

Ni–5 wt.% Al anodes for molten carbonate fuel cells (MCFCs) are fabricated using relatively cheap elemental powders instead of expensive alloy powders. The tape-cast green sheets are sintered in various atmospheres: reduction, full oxidation–reduction, and partial oxidation–reduction atmospheres. The anode sintered in a reduction atmosphere shows a morphology of a network structure of an Ni–Al solid solution with its surface covered with thin Al_2O_3 films, and has relatively low creep resistance. On the other hand, the anode sintered in a full oxidation–reduction atmosphere or the one sintered in a partial oxidation–reduction atmosphere has a morphology of small Al_2O_3 particles dispersed in a network structure. In the former, however, a large number of micropores are created during sintering. The latter does not have the micropore problem and generally exhibits high creep resistance. The highest creep resistance is shown by the anode sintered in a partial oxidation–reduction atmosphere with an oxidation time of 2.5 h.

Keywords: Molten carbonate fuel cell; Ni–5 wt.% Al anode; Creep resistance; Al_2O_3

1. Introduction

It was in the early 1980s that anode creep problem was recognised by many researchers and developers as one of the obstacles in the way of commercialisation of the molten carbonate fuel cell (MCFC). Anodes with sufficient structural and morphological stability are required for creep resistance, but the conventional nickel anodes did not meet this requirement [1]. Therefore, the nickel anodes had to be strengthened mechanically and such methods as solute-, precipitation-, or oxide-dispersion-strengthening were applied. Recent work has concentrated on the last mentioned method with the addition of oxidizable elements. The most commonly used additives are chromium and aluminium. Chromium in Ni–Cr anodes is lithiated after oxidation, however, to form $LiCrO_2$ and creates a considerable number of micropores in the process, which leads to the loss and redistribution of the electrolyte. So, the MCFC community is now paying increasing attention to Al, since, the Ni–Al system is not usually subject to the micropore problem and, moreover, generally shows higher creep resistance than the Ni–Cr system [2,3].

One of the attempts made by Ni–Al anode developers is to use a commercial Ni–5 wt.% Al alloy powder as the anode material and to enhance its creep resistance by producing Al_2O_3 dispersion during sintering. The solubility limit of Al in Ni is 5 wt.% and the underlying idea is to adopt both solute- and oxide-dispersion-strengthening. Unfortunately, however, the alloy powder is much more expensive than the Inco 255 Ni powder presently used as the basic material for the anode. In order to lighten the economic burden in mass production, we have established a process to fabricate using elemental powders an anode of the same composition and similar creep resistance as the one made from the alloy powder. A special focus is put on the sintering atmosphere because it strongly influences the morphology and eventually the creep behaviour of the anodes.

2. Experimental

Ni–5 wt.% Al anodes were fabricated using elemental powders of Ni (carbonyl-nickel type 255, Inco) and Al (High Purity Chemicals) as starting materials. The mean particle sizes of Ni and Al were 5 and 3 μm, respectively. The green sheets were prepared by tape casting using the procedure shown in Fig. 1. They were then sintered in various to determine the proper morphology for as high a creep resistance as possible at 1100 °C for 2 h in an H_2 (99.999% purity) atmosphere (called reduction atmosphere); or at 900 °C for 10 h in air and subsequently at 1100 °C for 3 h in an H_2

* Corresponding author. Tel.: +82-2-3290-3813; fax: +82-2-3290-3813.
E-mail address: gyubeom@yahoo.com (G. Kim).

0378-7753/02/$ – see front matter
PII: S0378-7753(01)00910-7

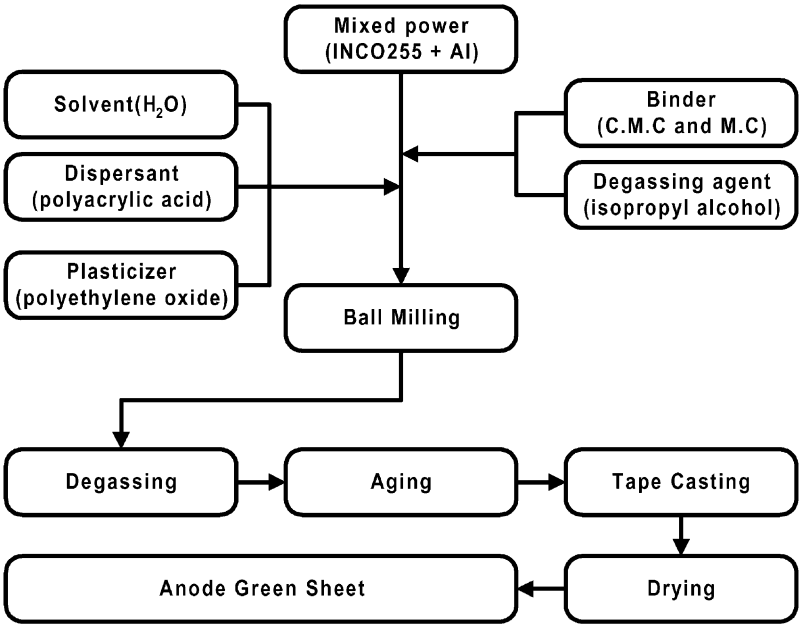

Fig. 1. Procedure for fabrication of anode green sheets by tape casting.

atmosphere (called full oxidation–reduction atmosphere); or at 900 °C for 2.5, 5, 7.5 or 10 h in an atmosphere of $P_{H_2}/P_{H_2O} = 10^{-2}$ and subsequently at 1100 °C for 3 h in an H_2 atmosphere (called partial oxidation–reduction atmosphere). A mixed gas of H_2/N_2 saturated with H_2O at 90 °C was used for the partial oxidation atmosphere and the ratio of P_{H_2}/P_{H_2O} was controlled by the flow rates of the H_2 and N_2 gases.

The sintered anode was characterised using an X-ray diffractometre (XRD, Rigaku Geigerflex DMAX-IIA) to identify the phases; a field emission scanning electron microscope (FE-SEM, Hitachi 6300), an energy dispersive X-ray spectrometer (EDX, Oxford), or an Auger electron spectrometer (AES, Physical Electronics 680) to study the morphology. The creep test was performed in the apparatus shown in Fig. 2 at a temperature of 650 °C and a pressure of 100 psi for 100 h in an H_2 atmosphere. Since, it is well known that the creep strain of a porous structure is a sensitive function of porosity, all the creep specimens were made to have porosities of a similar level so that their creep strains could be compared directly with one another. The porosity of the creep specimen was measured using the Archimedes method (ASTM, C373-72).

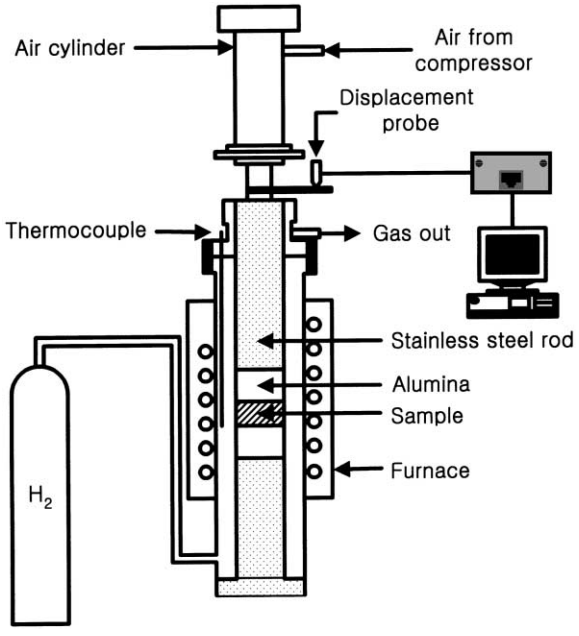

Fig. 2. Schematic diagram of apparatus used for creep tests.

3. Results and discussion

According to the phase diagram [4], Ni–Al alloys containing 5 wt.% Al are expected to exist as a single phase of Ni–Al solid solution in their equilibrium states. This can be confirmed by the XRD pattern of the Ni–5 wt.% Al anode sintered at 950 °C for 2 h in an H_2 atmosphere, see Fig. 3. This anode, however, contains a very small amount of Al_2O_3 when sintered at 1100 °C for 2 h in an H_2 atmosphere, which can also be seen in Fig. 3. A question therefore arises: why does Al oxidise in an H_2 atmosphere? This question can be answered in terms of the purity of the hydrogen gas. As already mentioned, the hydrogen gas used in this experiment was of 99.999% purity and nominally it contained 0.1 ppm of O_2 and 0.2 ppm of H_2O. So, this gas is supposed to make the atmosphere of $P_{H_2}/P_{H_2O} = 2.5 \times 10^6$ provided that all of the O_2 molecules in the gas has turned into H_2O by reaction with H_2. This might be still the oxidising atmosphere for Al at 1100 °C, but not quite at 950 °C.

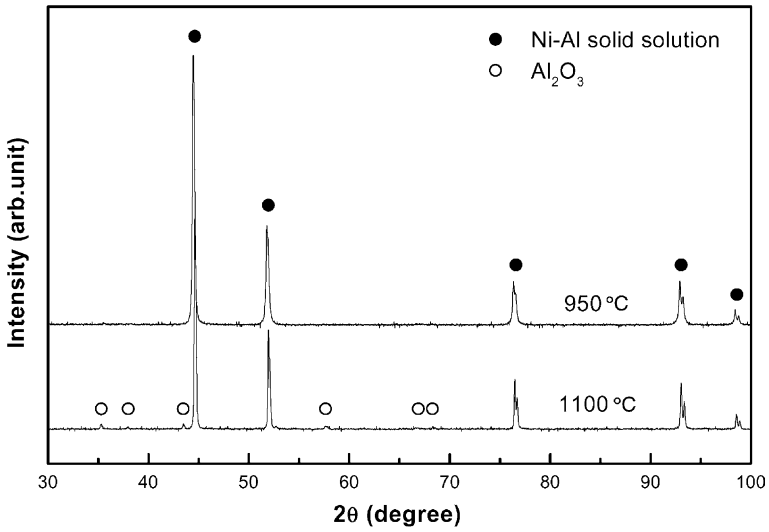

Fig. 3. XRD patterns of Ni–5 wt.% Al anodes sintered at 950 and 1100 °C for 2 h in an H_2 atmosphere.

A SEM and Al Kα dot map of the anode sintered at 1100 °C for 2 h in an H_2 atmosphere are shown in Fig. 4(a) and (b), respectively. In the micrograph, a typical network structure can be seen, but no Al_2O_3 particles. The reason why Al_2O_3 particles are not seen can be found in the dot map. According to the map, the H_2 atmosphere indeed oxidised Al, but in the form of a thin film which covered all of the surface of the network structure, not in the form of dispersed particles. A similar phenomenon has been observed for an Ni–12 wt.% Al anode in the form of an Auger depth profile [2] also obtained in our laboratory. The form of the thin Al_2O_3 film did not seem to be effective for sinter-resistance; hence, the porosity of this anode was found to be lower, 56% at most, than the typical value (>60%) usually obtained for the anodes of the same composition. The low sinter-resistance is expected to lead to low creep resistance. Indeed, the strain measured after a creep test performed on the anode of 56% porosity at 650 °C for 100 h was 4.1%. This value of creep strain certainly is much lower than the one of a pure nickel anode (>50%) [5], but is still too high for long-term operation of an MCFC. Furthermore, the value must have been much higher if the porosity of the anode were as high as the typical value for Ni–5 wt.% Al anodes.

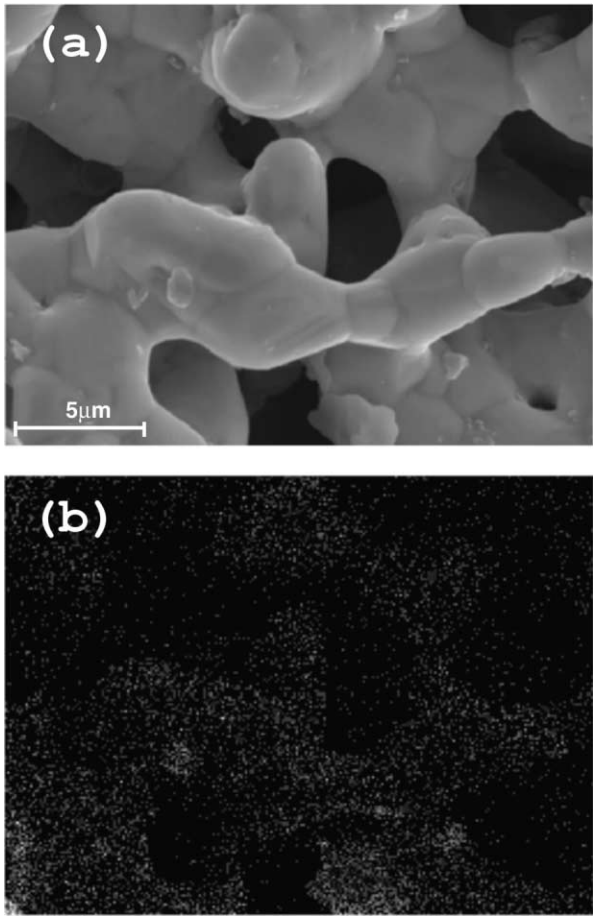

Fig. 4. (a) SEM image and (b) Al Kα dot map of Ni–5 wt.% Al anode sintered at 1100 °C for 2 h in an H_2 atmosphere.

The next attempt made for the purpose of Al_2O_3 dispersion was a full oxidation–reduction process. The green sheet was heated at 900 °C for 10 h in air so that Ni and Al could be fully oxidised, respectively, to NiO and Al_2O_3. It was then held at 1100 °C for 3 h in an H_2 atmosphere so that NiO could be reduced back to Ni. The XRD pattern of the anode after reduction is shown in Fig. 5. The peaks of both Ni–Al solid solution and Al_2O_3 phases can be identified. As can be seen in the SEM presented in Fig. 6, the Al_2O_3 phase in this anode exists in the form of small particles dispersed in the network structure of the Ni–Al solid solution, though the particles are not exposed on the surface but embedded in the structure. It can be concluded, however, from the pore-size distribution curve shown in Fig. 7 that this anode contains a large number of micropores. The micropores seem to have been created due to the large volume change during the Ni → NiO → Ni transformation and are known to give an

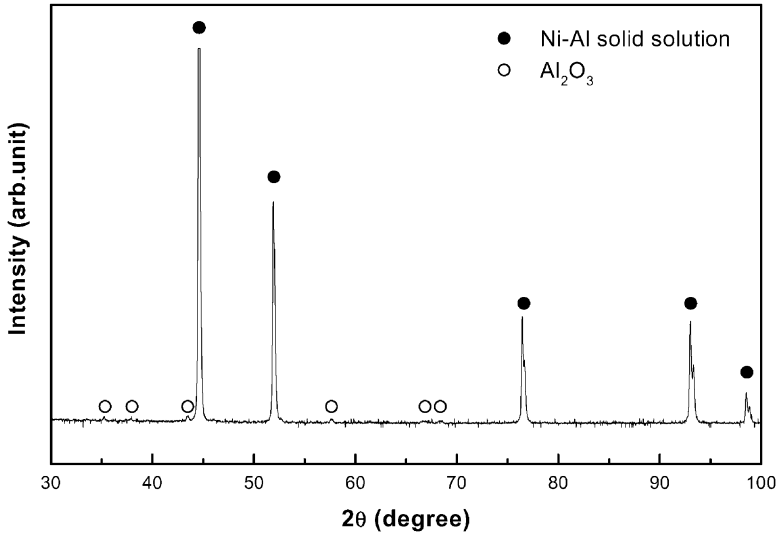

Fig. 5. XRD pattern of Ni–5 wt.% Al anode sintered at 900 °C for 10 h in air and subsequently at 1100 °C for 3 h in an H_2 atmosphere.

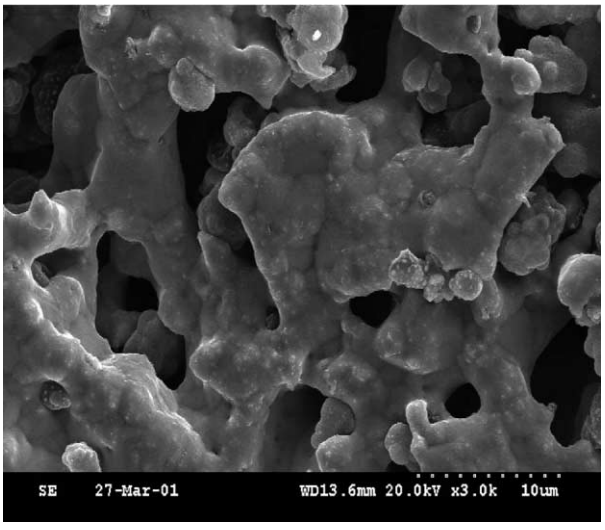

Fig. 6. SEM image of Ni–5 wt.% Al anode sintered at 900 °C for 10 h in air and subsequently at 1100 °C for 3 h in an H_2 atmosphere.

adverse effect on cell performance by redistribution of the electrolyte. Therefore, further investigation on this anode was deemed to be unnecessary.

To solve the micropore problem, we had to search in the Ellingham diagram [6] for the atmosphere that would oxidise Al, but not Ni, at 900 °C. We finally chose the one of $P_{H_2}/P_{H_2O} = 10^{-2}$ among many possibilities so that oxidation of Al should be guaranteed while oxidation of Ni could be barely avoided. The green sheet was then sintered at 900 °C for 2.5, 5, 7.5 and 10 h in the chosen atmosphere for partial oxidation. The XRD patterns of the anodes after partial oxidation are given in Fig. 8. While peaks of the Ni–Al solid solution phase are clearly seen, those of the Al_2O_3 phase are hardly discernible (though their positions are marked with arrows). This is probably because the amount of the Al_2O_3 phase is small and/or the particles are of such small size to induce extensive lin-broadening. Nevertheless, it can be clearly seen in the SEM images

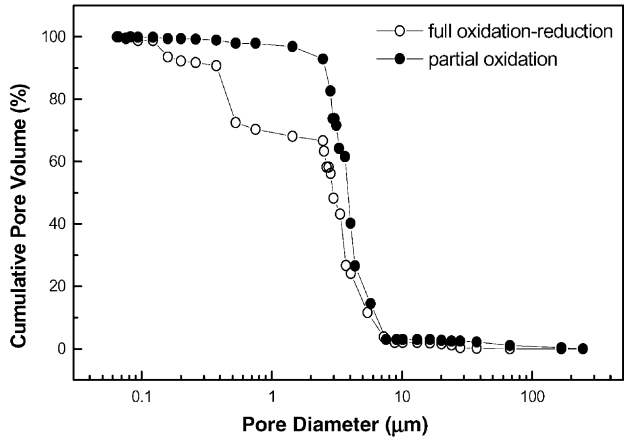

Fig. 7. Pore-size distributions for Ni–5 wt.% Al anodes prepared by full oxidation–reduction and partial oxidation–reduction processes.

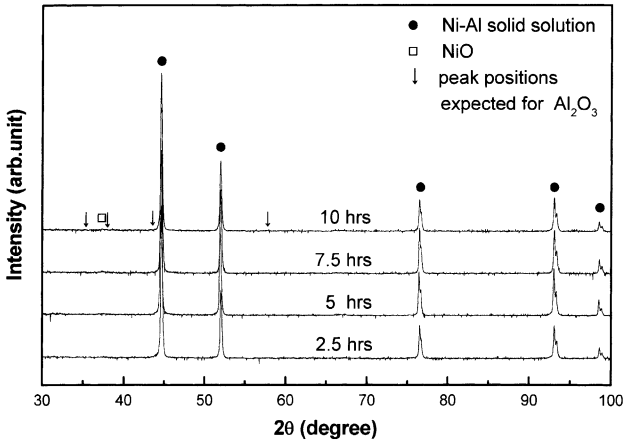

Fig. 8. XRD patterns of Ni–5 wt.% Al anodes sintered at 900 °C for various times in an atmosphere of $P_{H_2}/P_{H_2O} = 10^{-2}$.

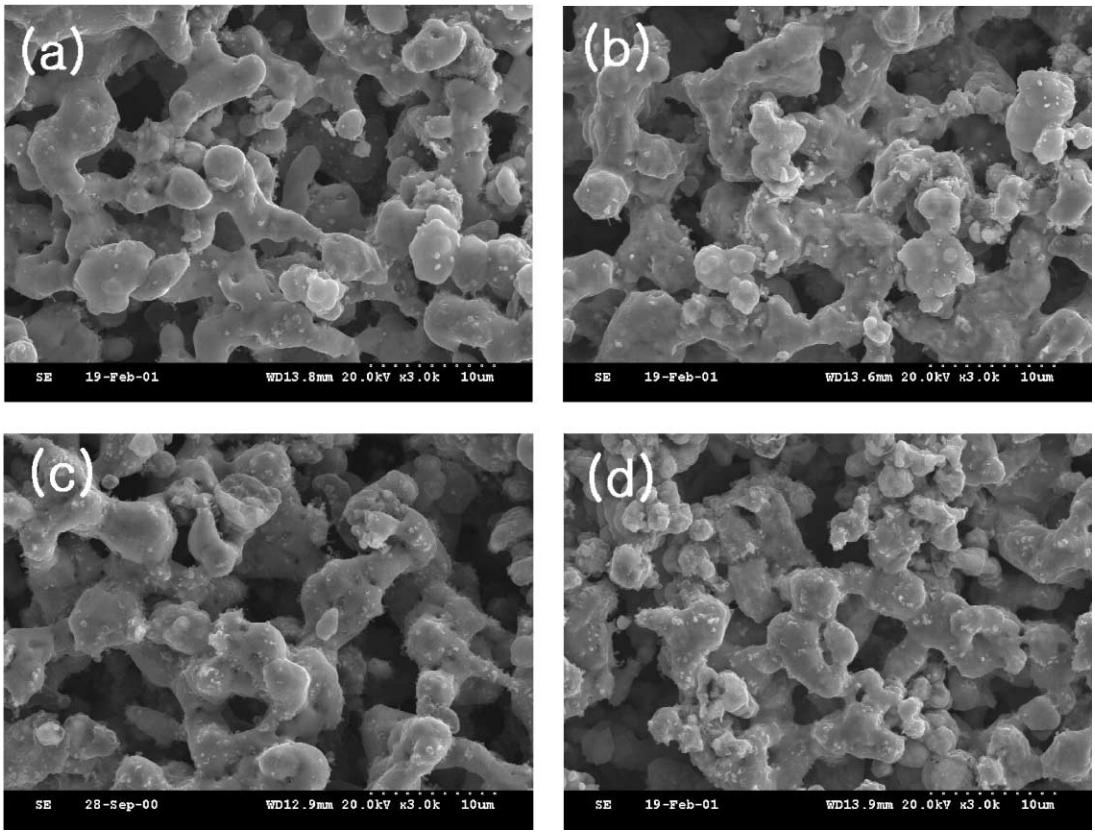

Fig. 9. SEM image of Ni–5wt.% Al anodes sintered at 900 °C for (a) 2.5, (b) 5, (c) 7.5, and (d) 10 h in an atmosphere of $P_{H_2}/P_{H_2O} = 10^{-2}$.

shown in Fig. 9 that very small particles are scattered on the surface of the network structure. These particles were subsequently found to be Al_2O_3. It can be also seen in Fig. 9 that the number of particles increases with time, but the particle size appears to be remained unaltered.

Another thing to notice in Fig. 8 is that, though not so clear to be observed immediately, a trace of a NiO peak is present at $2\theta \sim 37°$. The existence of the NiO phase can be confirmed by AES results Fig. 10(a) and (b) respectively show the scanning Auger microscope (SAM) image for the anode prepared by partial oxidation for 5 h, and the AES depth profile for the spot marked on the image. A very thin film of NiO can be identified in the depth profile. This unexpected oxide could have been formed due to a slight deviation of P_{H_2}/P_{H_2O} from the nominal value. Therefore, reduction of NiO to Ni was thought to be necessary and was performed under the same conditions as in the frill oxidation–reduction process, i.e. at 1100 °C for 3 h. The

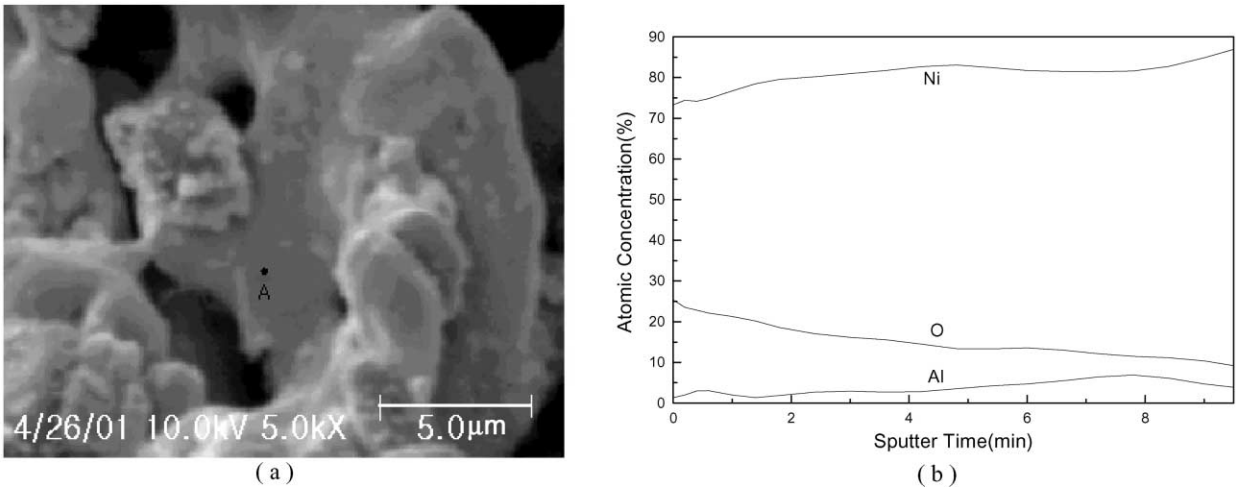

Fig. 10. (a) SAM image and (b) AES depth profile of Ni–5 wt.% Al anode sintered at 900 °C for 5 h in an atmosphere of $P_{H_2}/P_{H_2O} = 10^{-2}$.

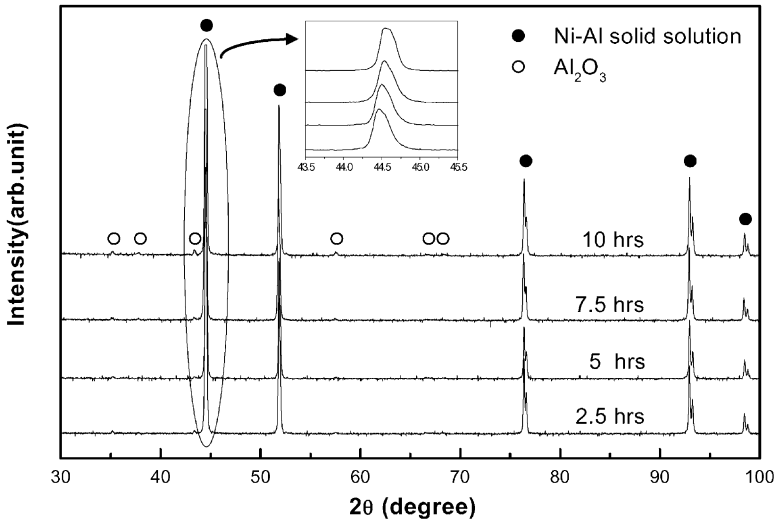

Fig. 11. XRD patterns of Ni–5 wt.% Al anodes sintered at 900 °C for various times in an atmosphere of $P_{H_2}/P_{H_2O} = 10^{-2}$ and subsequently at 1100 °C for 3 h in an H_2 atmosphere.

XRD patterns of the anodes after reduction are shown in Fig. 11. No trace of the above-mentioned NiO peak can be seen in the patterns. Al_2O_3 peaks, on the other hand, are more prominent than in Fig. 8 and become more distinct with time.

The inset of Fig. 11 shows the magnified view of the main peak of the Ni–Al solid solution phase at $2\theta \sim 44.5^\circ$ and it is clear that the peak shifts to the higher angle side as time increases, i.e. from 44.464° at 2.5 h to 44.542° at 10 h. In other words, the peak shifts towards the position for pure Ni, which is supposed to be 44.546° [7]. The lattice parameter a_0 of the cubic Ni–Al solid solution was calculated from the measured value of 2θ and plotted against oxidation time in Fig. 12. For the purposes of comparison, also included are a similar plot obtained from Fig. 8 for the anodes prepared by partial oxidation only, and the line marks for the lattice parameter of Ni [7] and that of Ni–5 wt.% Al solid solution calculated from the XRD pattern for a commercial alloy powder. Regardless of whether or not the reduction process has been carried out, a_0 decreases and approaches the value for pure Ni as time increases. Since, the atomic size of Al is definitely larger than that of Ni, the decrease in a_0, implies that a greater amount of Al in the solid solution has been oxidised and as a result the Al content in the solution gets smaller as time increases.

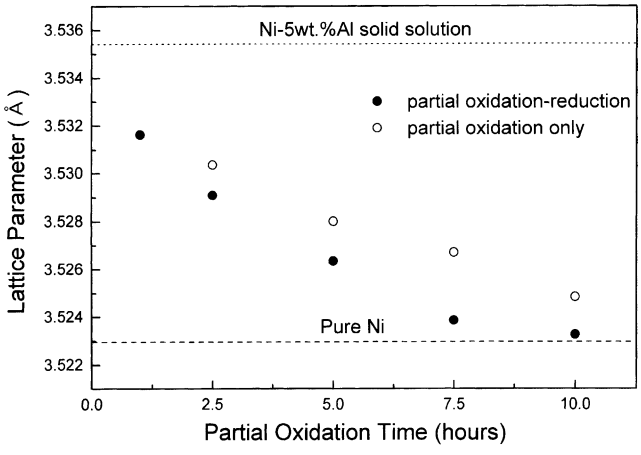

Fig. 12. Lattice parameters for Ni–5 wt.% Al anodes prepared by partial oxidation only and partial oxidation–reduction process.

It can be also concluded from the data in Fig. 12 that oxidation of Al continues during the reduction process as expected from the foregoing discussion on the purity of H_2 gas and, even though the experimental condition for the reduction process is identical no matter what the partial oxidation time is, the difference in lattice parameters before and after reduction increases, in other words the degree of oxidation during the reduction process increases, with increasing time. The SEM images of the anodes after reduction are shown in Fig. 13. They are slightly different from those before reduction (Fig. 9) in the sense that small particles are scattered on the surface of the network structure with similar densities. These particles are found to be Al_2O_3, as shown in Fig. 14(a) and (b) which, respectively, show the SEM image of the anode prepared by the partial oxidation–reduction process with an oxidation time of 10 h, and the Auger spectra for the two points marked on the image, one with a particle and the other without. A difference can be noticed after careful comparison of Figs. 9 and 13. The particle sizes generally appear larger after reduction than before. Therefore, it can be surmised that oxidation of Al during the reduction process might have been proceeded predominantly by growth of existing Al_2O_3 particles. This, together with the fact that the number of particles increases with oxidation time (Fig. 9), explains the increasing degree of oxidation during the reduction process with increasing oxidation time.

In summary, the reduction atmosphere produce the Al_2O_3 phase in the form of a thin film, while the (full or partial)

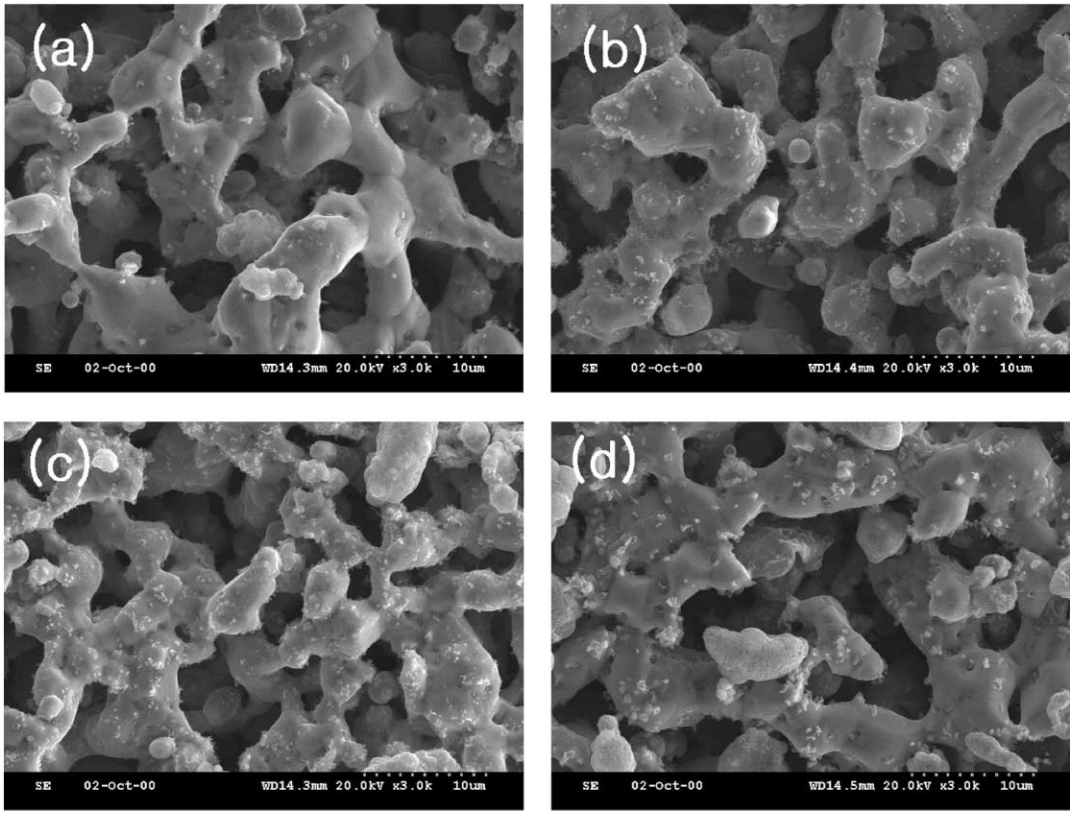

Fig. 13. SEM micrographs of Ni–5 wt.% Al anodes sintered at 900 °C for (a) 2.5, (b) 5, (c) 7.5 and (d) 10 h in an atmosphere of $P_{H_2}/P_{H_2O} = 10^{-2}$ and subsequently at 1100 °C for 3 h in an H_2 atmosphere.

oxidation–reduction atmosphere gave dispersed particles. A further question arises: what has made the morphologies of the Al_2O_3 phase different for various sintering atmospheres? To answer to this question, we searched for other differences produced by the two atmospheres than the morphology of Al_2O_3 phase and finally decided that the oxidation–reduction atmosphere oxidises Ni while the reduction atmosphere does not. From this, we drew a tentative conclusion that NiO must play some role for oxide dispersion. One possibility, as proposed by Haerig and Hofmann [8], is that, once both NiO and Al_2O_3 have been nucleated, the former grows much faster than the latter due to the higher diffusivity of Ni than that of Al, which suppresses the growth of the latter. If this proposition is correct, then the Al_2O_3 particles would be

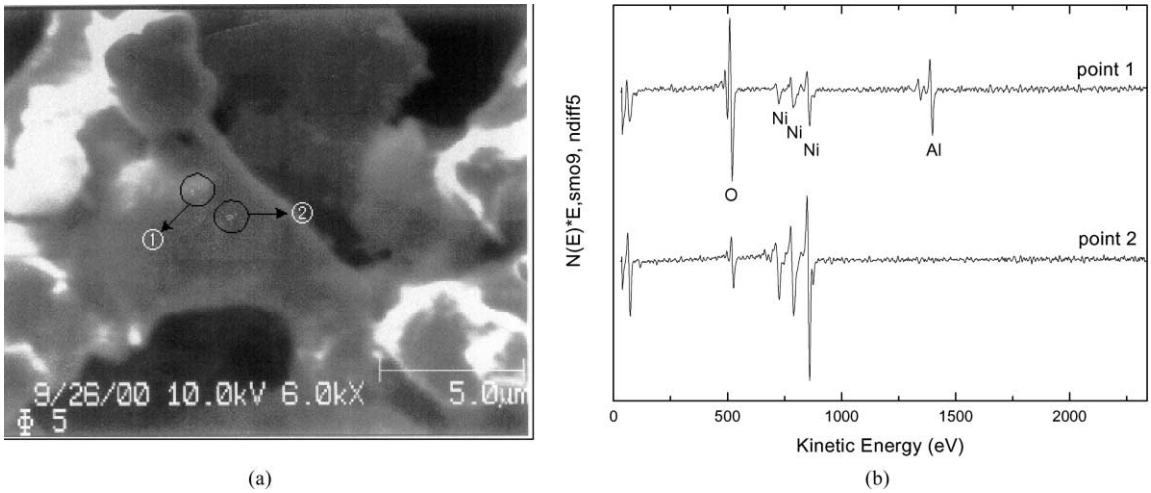

Fig. 14. (a) and (b) show the SEM image of the anode prepared by the partial oxidation–reduction process with an oxidation time of 10 h, and the Auger spectra for the two points marked on the image, respectively; one with a particle and the other without.

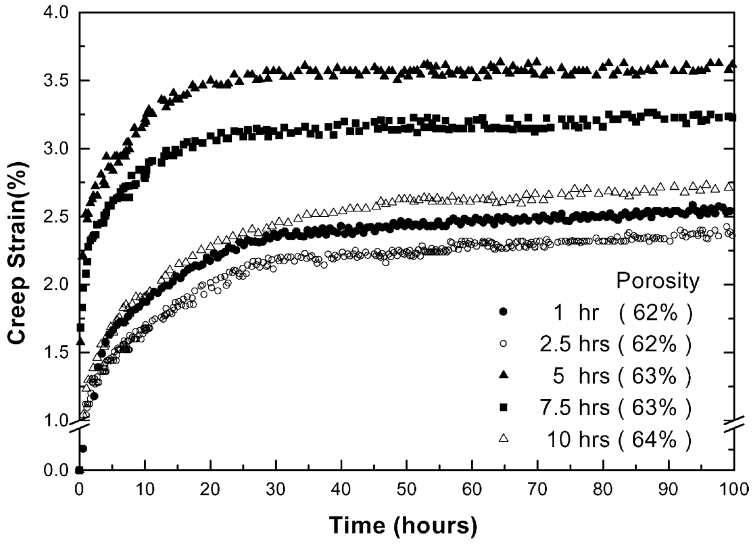

Fig. 15. Creep curves of Ni–5 wt.% Al anodes sintered at 900 °C for various times in an atmosphere of $P_{H_2}/P_{H_2O} = 10^{-2}$ and subsequently at 1100 °C for 3 h in an H_2 atmosphere.

covered with the fast-grown NiO phase in an actively Ni-oxidising environment such as a full oxidation–reduction atmosphere. This may be a reason why Al_2O_3 particles are not exposed on the surface but embedded in the network structure in the anodes sintered in full oxidation–reduction atmosphere.

The creep curves of the anodes sintered in a partial oxidation–reduction atmosphere for various oxidation times are shown in Fig. 15. As stated earlier, the porosities of the anodes were made similar so that a direct comparison of creep strains is possible. Unexpectedly, the creep strain after the 100 h-test is the lowest i.e. 2.3% at oxidation time of 2.5 h. The other values are 2.5% at 1 h, 3.6% at 5 h, 3.2% at 7.5 h and 2.7% at 10 h. The data for the oxidation time of 1 h is included for more detailed trend of creep strain variation with oxidation time. Thus, the creep resistance, the reciprocal of creep strain, undulates initially it goes through a maximum at 2.5 h and then a minimum at 5 h.

The anode sintered in a partial oxidation–reduction atmosphere can be considered as a composite of the Ni–Al solid solution and Al_2O_3 phases. Therefore, its creep resistance is supposed to be enhanced by combined contributions of solute- and oxide-dispersion-strengthening. As already shown in Fig. 12, the amount of the Al_2O_3 phase increases and the Al content in Ni–Al solid solution decreases with increasing oxidation time; in other words, the contribution of solute-strengthening to creep resistance decreases, whereas, the contribution of oxide-dispersion-strengthening increases with increasing oxidation time. Consequently, the creep resistance can be considered to be maximised some time in between, which happens to be 2.5 h. It is not yet known why the creep strain decreases again after 7.5 h but, even if so, a long-time process is not desirable for a low fabrication cost.

The pore-size distribution of the anode prepared by partial oxidation–reduction with oxidation time of 2.5 h is compared in Fig. 7 with that of an anode prepared by full oxidation–reduction. There is no sign of mircropore formation during sintering in the former. The electrical conductivity of this anode is 3.2×10^6 S m^{-1}, i.e. similar to the value for the Ni–10 wt.% Cr anode most frequently used for MCFCs.

4. Conclusions

Creep-resistant Ni–5 wt.% Al anodes for MCFCs are fabricated using elemental powders. The tape-cast green sheets are sintered under three different conditions, namely, at 1100 °C for 2 h in an H_2 atmosphere (reduction atmosphere); at 900 °C for 10 h in air and subsequently at 1100 °C for 3 h in an atmosphere (full oxidation–reduction atmosphere), or at 900 °C for 2.5, 5, 7.5 or 10 h in an atmosphere of $P_{H_2}/P_{H_2O} = 10^{-2}$ and subsequently at 1100 °C for 3 in an H_2 atmosphere (partial oxidation–reduction atmosphere). The effect of the atmosphere on the morphology and eventually the creep resistance of the anode has been investigated and the following conclusions can be drawn.

1. The anode sintered in a reduction atmosphere shows a morphology of a network structure of Ni–Al solid solution with its surface covered with thin Al_2O_3 films, and it has relatively low creep resistance.
2. The anode sintered in a full oxidation–reduction atmosphere exhibits a morphology of a network structure dispersed with Al_2O_3 particles. This anode was judged to be inadequate for actual use, however, since it contains large numbers of micropores created during sintering.
3. The anode sintered in a partial oxidation–reduction atmosphere also has a morphology of a network structure dispersed with Al_2O_3 particles. The amount of the Al_2O_3 phase increases and the Al content in the

Ni–Al solid solution decreases with increasing oxidation time. Accordingly, the creep resistance is highest at an oxidation time of 2.5 h when the combined contributions of solute- and oxide-dispersion-strengthening are considered to be maximised.

Acknowledgements

This study was financially supported by The Korea Electric Power Corporation and by The Korea Ministry of Commerce, Industry and Energy.

References

[1] K. Kordesch, G. Simader, Fuel Cells and Their Applications, VCH, New York, 1996, pp. 111–133.
[2] H.K. Yoon, N.J. Kim, D.Y. Lee, H.C. Lim, J. Kor. Inst. Met. Mater. 38 (4) (2000) 534.
[3] C.D. Iacovangelo, J. Electrochem. Soc. 133 (1986) 2410.
[4] E.A. Brandes, G.B. Brook (Eds.), Smithells Metals Reference Book, 7th Edition, Butterworth–Heinemann, Oxford, 1992, pp. 11–44.
[5] D. Lee, J. Kim, J. Inst. Ind. Tech. Korea Univ. 31 (1995) 11.
[6] D.R. Gaskell, Introduction to Metallurgical Thermodynamics, 2nd Edition, McGraw-Hill, New York, 1981, p. 287.
[7] JCPDS card 44-1159.
[8] M. Haerig, S. Hofmann, Appl. Surf. Sci. 125 (1998) 99.